

Review article

Diagnostic and Prognostic Value of CMR T₁-Mapping in Patients With Heart Failure and Preserved Ejection Fraction



Karl-Philipp Rommel,^a Christian Lücke,^b and Philipp Lurz^{a,*}

^a Department of Internal Medicine/Cardiology, Heart Center, University of Leipzig, Leipzig, Germany

^b Department of Radiology, University of Leipzig, Heart Center, Leipzig, Germany

Article history:

Available online 15 March 2017

Keywords:

Cardiac magnetic resonance
Heart failure with preserved ejection fraction
Diastolic dysfunction
T₁ mapping

Palabras clave:

Resonancia magnética cardiaca
Insuficiencia cardiaca con fracción de eyección conservada
Disfunción diastólica
Mapeo T₁

ABSTRACT

Heart failure with preserved ejection fraction (HFpEF) presents a major challenge in modern cardiology. Although this syndrome is of increasing prevalence and is associated with unfavorable outcomes, treatment trials have failed to establish effective therapies. Currently, solutions to this dilemma are being investigated, including categorizing and characterizing patients more diversely to individualize treatment. In this regard, new imaging techniques might provide important information. Diastolic dysfunction is a diagnostic and pathophysiological cornerstone in HFpEF and is believed to be caused by systemic inflammation with the development of interstitial myocardial fibrosis and myocardial stiffening. Cardiac magnetic resonance (CMR) T₁-mapping is a novel tool, which allows noninvasive quantification of the extracellular space and diffuse myocardial fibrosis. This review provides an overview of the potential of myocardial tissue characterization with CMR T₁ mapping in HFpEF patients, outlining its diagnostic and prognostic implications and discussing future directions. We conclude that CMR T₁ mapping is potentially an effective tool for patient characterization in large-scale epidemiological, diagnostic, and therapeutic HFpEF trials beyond traditional imaging parameters.

© 2017 Sociedad Española de Cardiología. Published by Elsevier España, S.L.U. All rights reserved.

Valor diagnóstico y pronóstico del mapeo de T₁ mediante RMC de los pacientes con insuficiencia cardiaca y fracción de eyección conservada

RESUMEN

La insuficiencia cardiaca con fracción de eyección conservada (ICFec) es un reto para la cardiología moderna. Aunque este síndrome, de prevalencia cada vez mayor, se asocia a resultados desfavorables, los ensayos de tratamientos no han logrado establecer terapias eficaces. Actualmente se investigan soluciones a este problema, como categorizar y caracterizar a los pacientes de manera más diversificada en un intento de individualizar los tratamientos. En este campo, las nuevas técnicas de imagen aportan información importante. La disfunción diastólica es la piedra angular del diagnóstico y la fisiopatología de la ICFec, y se considera que puede tener origen en la fibrosis intersticial y la rigidez del miocardio secundaria a inflamación sistémica. Las técnicas de mapeo de T₁ mediante resonancia magnética cardiaca (RMC) constituyen una nueva herramienta que permite el diagnóstico no invasivo de la fibrosis miocárdica difusa en el espacio extracelular. Esta revisión ofrece una visión general sobre el potencial de caracterizar mediante RMC con mapeo T₁ el miocardio de los pacientes con ICFec, subrayar sus implicaciones diagnósticas y pronósticas y tratar de las direcciones futuras. Se concluye que la técnica de mapeo T₁ mediante RMC podría ser un instrumento eficaz para la caracterización de los pacientes en estudios epidemiológicos, diagnósticos y terapéuticos amplios sobre ICFec.

© 2017 Sociedad Española de Cardiología. Publicado por Elsevier España, S.L.U. Todos los derechos reservados.

* Corresponding author: Department of Internal Medicine/Cardiology, Struempellstrasse 39, 04289 Leipzig, Germany.
E-mail address: Philipp.Lurz@gmx.de (P. Lurz).

Abbreviations

CMR: cardiac magnetic resonance
 ECV: extracellular volume
 EDPVR: end-diastolic pressure volume relation
 HFpEF: heart failure with preserved ejection fraction
 HFrEF: heart failure with reduced ejection fraction
 MOLLI: modified look-locker inversion-recovery

INTRODUCTION

The prevalence of patients presenting with heart failure (HF) with preserved ejection fraction (HFpEF) is increasing and already accounts for half of the HF population.^{1,2} Contrary to the initial belief of a rather benign entity, the occurrence of HFpEF is now known to be associated with significant morbidity and mortality, similar to that patients with heart failure and reduced ejection fraction (HFrEF).³

While therapeutic strategies of the latter patient group have undergone multiple advances in the last 3 decades and large outcome trials have demonstrated mortality benefits,⁴ for HFpEF patients the validation of an effective treatment option is pending.

The paucity of positive outcome trials in HFpEF has been attributed to the heterogeneity of included patients.⁵ Although left ventricular (LV) diastolic dysfunction had been proposed as the pathophysiological cornerstone of the HFpEF syndrome, only recently have consensus criteria been established for the diagnosis of these patients.⁶ Importantly, these include morphological evidence of impaired LV diastolic function, mainly relying on echocardiographic evaluation. Conversely, clinical HFpEF trials have included about one third of patients with normal diastolic function,^{7,8} while up to two thirds of patients showed impaired systolic function.⁹ Multiple alternative impairments in cardiac, vascular, and peripheral function have been identified, which can coexist with one another, and eventually lead to different predominant triggers of HF symptoms.^{10–17}

Successfully addressing the complexity of the HFpEF syndrome is mandatory for establishing tailored, personalized therapies. A solution to this problem has been suggested in the form of stratification according to the clinical presentation,¹⁸ the involved comorbidities⁵ or even to more complex phenotypic maps created by machine-learning algorithms.¹⁴

In clinical practice, cardiac imaging is indispensable for diagnosing and assessing HFpEF patients, as well as for excluding differential diagnosis.¹⁹ New imaging techniques might provide possibilities to better characterize HFpEF patients. Cardiac magnetic resonance (CMR) imaging has become increasingly available and is well established in the evaluation of cardiac morphology and function. Diastolic function can be assessed by flow, strain and volume-time-curve measurements, similar to other imaging techniques, such as echocardiography or nuclear imaging. In contrast to other imaging techniques, CMR can also provide information on myocardial tissue composition, given its high spatial resolution and its molecular source of imaging signal.²⁰ The late gadolinium enhancement (LGE) technique has convincingly been shown to be able to depict and quantify focal myocardial fibrosis. The presence of LGE has proven relevant in the prognosis of a number of cardiovascular conditions.^{21–23} However, LGE depicts mainly focal pathologies, but is less suitable to assess diffuse alterations such as fibrosis. The assessment of T₁ relaxation times by CMR T₁ mapping is a novel emerging technique for quantitative tissue characterization, with the ability to detect

interstitial/diffuse myocardial fibrosis, histologically validated in a wide spectrum of conditions.^{24,25}

The current understanding of the HFpEF syndrome relies on the concept that multiple comorbidities create a systemic inflammatory state.²⁶ This (subclinical) inflammation affects multiple organ systems. In the myocardium, a signaling cascade leads to reactive interstitial fibrosis and altered paracrine communication between endothelial cells and surrounding cardiomyocytes. As a result, myocardial stiffness increases, which in turn leads to diastolic dysfunction with elevations in LV filling pressures.²⁷

Therefore, fibrosis quantification is of great interest in HFpEF patients and implies the potential of CMR imaging to provide information on myocardial tissue composition and to identify patients who might benefit from antifibrotic therapies. Accurate quantification of diffuse myocardial fibrosis has the potential to guide the diagnosis and monitoring of HFpEF as well as to serve as a measure of success of future treatment strategies.

In the present review, we provide an overview of noninvasive myocardial tissue characterization with CMR T₁ mapping in HFpEF patients, outlining its diagnostic and prognostic implications and discussing future directions.

HEART FAILURE WITH PRESERVED EJECTION FRACTION

Heart failure with preserved ejection fraction is increasingly recognized as a complex syndrome, occurring in association with advanced age and cardiovascular, metabolic, and proinflammatory comorbidities.²⁶ Ultimately, patients with HFpEF demonstrate impaired LV relaxation and increased diastolic LV stiffness.²⁸

Increased LV stiffness suggests passive myocardial stiffening attributable to fibrosis and altered cardiomyocyte function. Endomyocardial biopsy studies in HFpEF demonstrate myocyte hypertrophy, interstitial fibrosis, incomplete myocardial relaxation, and increased cardiomyocyte stiffness, as well as evidence of systemic inflammation and oxidative stress.^{29–33} These observations led to a new paradigm for the pathophysiology of HFpEF. Theory holds that comorbidities create a systemic proinflammatory milieu, coronary microvascular endothelial inflammation, production of profibrotic cytokines, and subsequent development of interstitial fibrosis. Additionally, oxidative stress limits nitric oxide bioavailability and decreases protein-kinase-G mediated cellular processes. This leads to a hypophosphorylation of proteins that influence myofiber relaxation and stiffness, further impairing LV diastolic function.²⁶ Recently, a fairly large autopsy study (124 HFpEF and 104 controls) has provided evidence to support this concept, as Mohammed et al.³⁴ found that HFpEF patients showed significantly more myocardial hypertrophy and fibrosis, which was related to microvascular rarefaction rather than arterial hypertension.

Although diastolic dysfunction is the most prevalent and typical pathophysiological finding in patients with HFpEF, impairments in multiple systems render it a complex syndrome. Abnormalities in LV systolic function, right-heart function, the vasculature, endothelium, and the periphery (including skeletal musculature) play important roles. Furthermore, HFpEF patients present with impaired cardiac reserve function, namely the ability to enhance arterial, chronotropic, and LV systolic, and diastolic performance with exercise.^{10–17} Chronic elevation of LV filling pressures leads to left atrial (LA) remodeling and dysfunction, mixed pulmonary hypertension, and, ultimately, right ventricular (RV) remodeling and dysfunction. Indeed, RV systolic dysfunction is a major predictor of outcome in the HFpEF population, whereas the impact of RV dysfunctionality in patients with preserved biventricular systolic function, requires further elucidation.^{16,17} However, the

model of disease progression in HFpEF is less clear than in HFrEF with significant heterogeneity in phenotypic expression.

Echocardiography is a widely available and cost-effective technique with high temporal resolution, providing a convenient tool for initial assessments.²⁶ However, many of the derived parameters are load-dependent and may mislead clinical judgement.³⁵

The gold standard for measuring diastolic filling pressures remains invasive cardiac catheterization. Using high-fidelity conductance catheters, the pressure and volume of the LV can be measured simultaneously. This approach allows the assessment of a number of systolic and diastolic functional parameters: Tau, the time constant of pressure-decay during isovolumic relaxation, characterizes early diastolic relaxation. Beta, the passive stiffness constant, characterizes the end-diastolic pressure-volume relationship.^{13,36}

Whereas the former is thought to be a consequence of an impaired active process of muscular inactivation, asynchronous contraction, or pathological loading conditions,³⁷ the latter is attributed to an increase in myocardial stiffness as detailed above. Both mechanisms have been demonstrated to play a major role in the development of HFpEF and possibly suggest different treatment targets²⁸ (Figure 1).

CARDIAC MAGNETIC RESONANCE T₁ MAPPING

A fundamental principle of magnetic resonance imaging is that the signal intensity of pixels is based on the relaxation of hydrogen nuclei protons in a static magnetic field, providing a sensitive soft tissue image contrast to tissue composition, which can be a reflection of physiology and pathophysiology.¹⁹ T₁ relaxation times reflect the course of longitudinal magnetization recovery, after it was disturbed from its equilibrium state by applying a radiofrequency pulse to invert the magnetization. Traditionally, T₁ relaxation properties are encoded in the pixel intensities of images and can identify focal pathologies in the myocardium, such as acute myocardial infarction or areas of replacement fibrosis in comparison to surrounding reference tissue (T₁ weighting). Recent advances now allow numerical quantification of T₁ relaxation times in the heart. The resulting T₁ maps can be color encoded and contain information on T₁ times in each voxel, making it feasible to detect and quantify even relatively small variations of T₁ times within the myocardium to highlight tissue pathology.³⁸ With the incorporation of the administration of extracellular paramagnetic contrast agent (gadolinium), it is possible to further enhance the detection of (extracellular) tissue abnormalities.³⁹ Moreover, the

extracellular volume (ECV) fraction can be calculated, providing information on the relative expansion of the extracellular matrix, thus providing a noninvasive alternative to myocardial biopsy studies.²⁴

TECHNIQUES

The rate at which the spin magnetization recovers its equilibrium state depends on tissue characteristics and the presence of contrast agents. The time course of T₁ relaxation is generally approximated by an exponential function. The general principle for T₁ mapping is to acquire multiple images at different time points after inversion or nulling of the equilibrium magnetization with radiofrequency pulses to fit the T₁ curve to the signal intensities of a voxel of the images to assess the equation for T₁ relaxation.³⁸

Multiple varieties of this basic inversion recovery (IR) sequences have been used, including the standard LL (look-locker) sequence,⁴⁰ the modified LL inversion-recovery (MOLLI) sequence,⁴¹ and the shortened MOLLI (ShMOLLI) sequence.⁴² Alternatively, saturation recovery (SR) techniques, such as the saturation recovery single-shot acquisition sequence (SASHA), can be used, which rely on actively nulling the longitudinal magnetization at different time points to estimate the fit of the T₁ relaxation curve.⁴³ Additionally, combined IR-SR sequences exist (SAPPHIRE). While all these techniques have been shown to be reproducible and diagnostically feasible, they differ in terms of breath hold duration, motion artifact susceptibility, heart rate dependency, signal-to-noise ratio, accuracy, and precision.⁴⁴ Less frequently, other sequences or modifications have been used for T₁ mapping, including continuous readout using Fast Low Angle SHot (FLASH-IR), 2-dimensional spin-and-stimulated-echo-planar imaging (ss-SESTEPI), variable k-space sampling (VAST), and 3-dimensional phase-sensitive inversion-recovery (PSIR).^{45–48} By way of example, we describe here the most widely used clinical technique for T₁ mapping to date, the MOLLI sequence (Figure 2). During diastole single-shot, images are acquired intermittently during 3 heartbeats after the first 2 IR pulses and 5 beats after the third IR pulse with 3 recovery beats in between, also denoted 3(3)3(3)5 (number of acquired pictures [number of recovery beats]). Thus, multiple points along the T₁ recovery curve can be acquired. The MOLLI technique and its variations, like 3(3)5 or 5(3)3(3)3, have been shown to be highly reproducible and yield source images with a high signal-to-noise ratio, with a lower heart rate dependency with the 5(3)3(3)3, compared to the 3(3)5 approach.⁴⁹

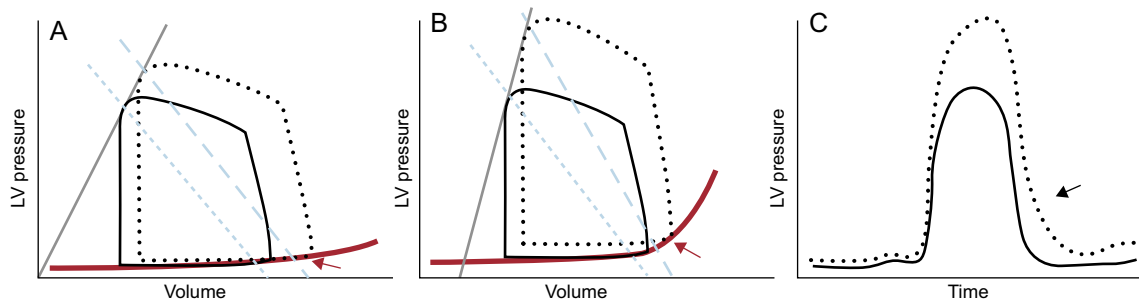


Figure 1. Left ventricular (LV) pressure-volume-loops of control patients (panel A) and heart failure with preserved ejection fraction patients (panel B) at rest (solid lines) and during exercise (dotted lines) demonstrating an increased arterial elastance (slope of dashed blue lines), as a surrogate for arterial stiffening, and an elevated slope of the end-diastolic pressure volume relationship, indicating ventricular stiffening (thick red line). Marked elevation of afterload with exercise leads to prolongation of the LV pressure decay during isovolumic relaxation in heart failure with preserved ejection fraction patients (panel C, black arrow). In combination with increased ventricular stiffness, this leads to elevated end-diastolic pressures and a pathological rise of the end-diastolic pressure volume relations (red arrows, panels A and B).

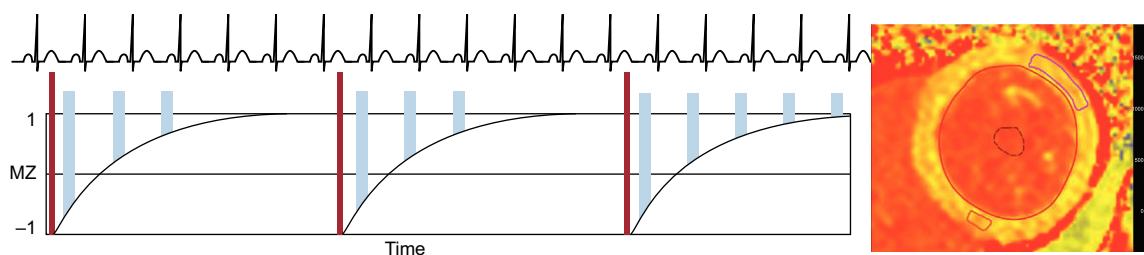


Figure 2. Acquisition strategy for T_1 -mapping using a MOLLI sequence. After an inversion pulse (thin dark blue bars), image read outs (wide yellow bars) are performed in diastole over 3 heartbeats, followed by a rest period of 3 heartbeats. Subsequently, another inversion with read outs with a slight offset is performed over another 3 heartbeats. Finally, read outs over 5 beats are acquired after a 3-beat recovery period. This MOLLI scheme is therefore termed 3(3)3(3)5. By fitting the signal intensity of each pixel to the T_1 recovery curve, a T_1 map (right image) can be generated. MOLLI, modified look-locker inversion-recovery.

EXTRACELLULAR VOLUME FRACTION

Dividing the myocardium in intra- and ECV, the intracellular compartment comprises myocytes, fibroblast, endothelial cells and smooth muscle cells, while ECV can be further divided into a vascular component (blood) and the residual interstitial space, including fibrous connective tissue, edema and inflammatory infiltration. Changes in ECV are generally thought to be predominantly driven by changes in the interstitial space.³⁸ Administration of an extracellular gadolinium-based contrast agent has been shown to be sensitive to increased extracellular volume associated with diffuse myocardial fibrosis. However, a single postcontrast T_1 measurement has limitations due to a variety of confounding factors, such as gadolinium clearance rate, time of measurement, injected dose, body composition, and hematocrit.²¹ These

limitations can be partly overcome by direct measurement of the changes in T_1 of the myocardium, related to changes in blood pool T_1 before and after contrast administration.³⁹ When corrected for hematocrit, the myocardial extracellular fractional distribution, can be quantified as ECV according to the formula (Figure 3):

$$ECV = (1 - \text{hematocrit}) \cdot \frac{\left(\frac{1}{T_{1 \text{ myocardium postcontrast}}} - \frac{1}{T_{1 \text{ myocardium native}}} \right)}{\left(\frac{1}{T_{1 \text{ blood pool postcontrast}}} - \frac{1}{T_{1 \text{ blood pool native}}} \right)}$$

DETECTION OF DIFFUSE MYOCARDIAL DISEASE

When interpreting T_1 times for the detection of diffuse cardiac disease, a number of considerations should be kept in mind. The

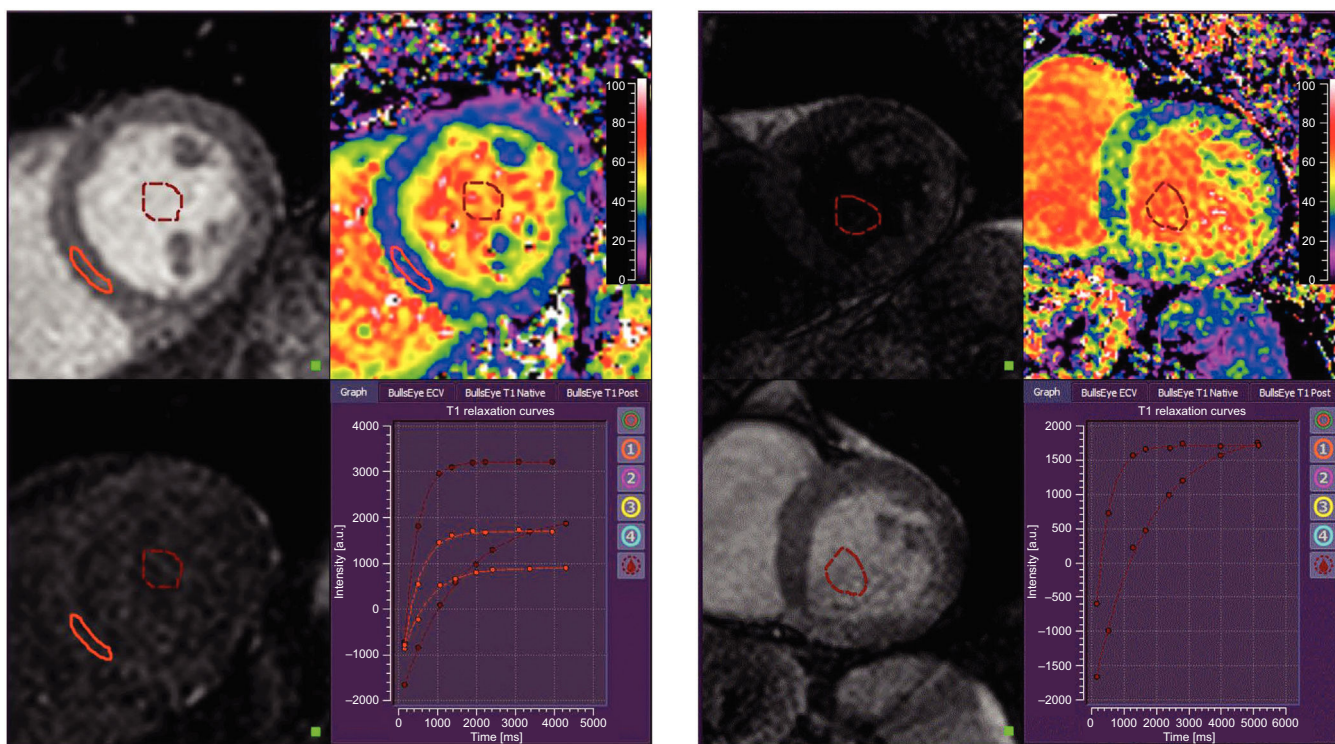


Figure 3. Extracellular volume maps derived from quantification of the change of T_1 times in the myocardium and blood pool before and after administration of gadolinium contrast, corrected for the hematocrit. On the left, a healthy control participant demonstrates a low global extracellular volume fraction of 22%. On the right, a patient with heart failure with preserved ejection fraction is illustrated, who demonstrates diffuse changes in the myocardial T_1 signal with an elevated global extracellular volume fraction of 36%.

CMR signal for noncontrast (native) T_1 times depends on both intracellular and extracellular factors, with more myocardial fibrosis and inflammation yielding higher values, while myocardial iron and fat accumulation shorten native T_1 times. Postcontrast T_1 times are predominantly reflective of changes in the extracellular space, as accumulating extracellular contrast agent shortens the T_1 values.³⁸ Importantly, morphological features other than fibrosis might influence T_1 measures to a variable extent, such as the presence of myocardial inflammation with intra- and extravascular edema and hyperemia.^{50,51}

Nevertheless, a consistent relationship between the three T_1 indices (native T_1 , postcontrast T_1 , and ECV) and the extent of biopsy proven diffuse myocardial fibrosis has been reported in various conditions, including aortic stenosis, hypertrophic cardiomyopathy, and heart failure. Overall, there is considerable variation among observed relationships, with ECV demonstrating the best correlations with fibrosis (Pearson $r = 0.49$ – 0.98).²⁴

The determination of T_1 indices also provides prognostic information in a variety of cardiovascular diseases with regards to the prediction of all-cause mortality and composite endpoints with heart failure admissions.^{46,52–56} These studies outline the ability of CMR imaging to noninvasively characterize the myocardium, allowing quantification of the burden of diffuse disease, which is linked to adverse outcomes.

Unfortunately, the susceptibility of CMR mapping techniques to only subtle changes in imaging techniques and vendor standards hampers direct comparisons of results between trials and implies the need to establish a range of reference T_1 values at each institution according to their specific protocol.⁴⁹ However, efforts are underway to standardize T_1 measurements.^{57,58}

T_1 MAPPING IN HEART FAILURE WITH PRESERVED EJECTION FRACTION

As described previously, in HFpEF, comorbidities promote a systemic inflammatory state, leading to cellular stiffening and the occurrence of reactive interstitial fibrosis, eventually leading to diastolic dysfunction.²⁶

In line with these considerations, abnormal T_1 values have been demonstrated in conditions known to be associated with myocardial fibrosis (hypertrophic cardiomyopathy, amyloidosis, and diabetic cardiomyopathy), relating to echocardiographically-determined indices of impaired diastolic function.^{59–61}

Not surprisingly, increased attention is being paid to CMR T_1 mapping in HFpEF patients, although overall data are still limited.

Su et al.⁶² evaluated 62 HFpEF patients, 40 HFrEF patients and 22 hypertensive controls with CMR T_1 mapping using a MOLLI scheme. Since they aimed to investigate the rate of diffuse fibrosis, areas of focal scarring were manually excluded, an important consideration, given that a significant percentage of the HFrEF group had ischemic heart diseases. They found that ECV was significantly elevated in HFpEF patients (median 29%) compared with control patients (median 28%) but significantly lower compared with HFrEF patients (median 31%). Ventricular function was evaluated using a volume-time curve approach derived from CMR cine imaging, providing information on the peak ejection and peak filling rates for systolic and diastolic function, respectively. Peak filling rates were significantly reduced in patients with HFrEF and were reduced to a lesser extent in patients with HFpEF. Interestingly, ECV was correlated with peak filling rates in the HFpEF group but not in the controls or those with HFrEF. Additionally, systolic ventricular function indices correlated with ECV in HFpEF patients. While native T_1 times did not differ, postcontrast T_1 showed a distribution similar to ECV between groups. Limitations related to the inclusion criteria, not

representing the current definition of HFpEF patients, the lack of echocardiographic data, and the use of highly load-dependent and therefore rarely used ventricular functional indices. However, the study elegantly suggested a strong connection between CMR-derived myocardial fibrosis quantification and altered ventricular function in HFpEF.

Insights into the prognostic value of T_1 mapping in HFpEF patients come from Mascherbauer et al.^{46,63} In 1 study, HFpEF was clinically suspected in 100 individuals and was confirmed in 63 by a guideline-recommended algorithm incorporating echocardiography, B-type natriuretic peptide measures, and right heart catheterization.⁴⁶ All patients underwent noninvasive characterization with T_1 mapping using a FLASH-IR sequence and gadolinium contrast administration; among the 61 individuals with confirmed HFpEF who also had interpretable T_1 images, 16 combined cardiac outcome events occurred (3 deaths from cardiovascular cause and 13 hospitalizations for heart failure) during a mean follow-up period of 22.9 ± 5.0 months. Postcontrast T_1 times (hazard ratio [HR], 0.99; 95% confidence interval [95%CI], 0.98–0.99); $P = .046$), LA area > median (HR, 1.08; 95%CI, 1.03–1.13; $P < .01$) and pulmonary vascular resistance (HR, 1.00; 95%CI, 1.00–1.01; $P = .03$) were independently associated with the combined endpoint. Additional insights were gained through endomyocardial biopsies in 9 patients. Interestingly, semiautomatically quantified extracellular volume matrix correlated extremely well with postcontrast T_1 times in HFpEF patients ($r = 0.98$; $P < .01$). Conversely, no relation between T_1 times and collagen content could be identified. These findings again highlight that T_1 estimation of ECV may overestimate diffuse fibrosis because it is also modulated by other factors beyond fibrosis. Comparison of HFpEF patients and patients not classified as having HFpEF yielded shorter postcontrast T_1 times ($P < .01$) and a slightly lower (though normal) LV ejection fraction. Of note, T_1 times also correlated with pulmonary vascular resistance and RVEF, suggesting a link between extracellular matrix deposition and the development of adverse pulmonary hemodynamic remodeling in HFpEF.

In the most recent work by the same group, 117 patients diagnosed on the basis of the current European Society of Cardiology consensus criteria⁶ were thoroughly investigated including right heart catheterization, echocardiography, 6-minute walk test, and LV myocardial biopsy in 18 patients.⁶³ Contrast-enhanced T_1 mapping with determination of ECV was performed using a 5(3)3 precontrast and 4(1)3(1)2 postcontrast MOLLI sequence. Heart failure with preserved ejection fraction patients were found to have higher ECV ($n = 117$, $29\% \pm 4\%$) than the local reference group ($n = 35$, $25\% \pm 3\%$; $P < .01$) of healthy controls. In the HFpEF cohort, ECV correlated fairly well with histology-proven extracellular matrix ($r = 0.49$; $P = .04$) and poorly but significantly with clinically important parameters associated with HFpEF, such as the E/A ratio ($r = 0.25$), right atrial pressure ($r = 0.21$), stroke volume ($r = -0.20$), n-terminal prohormone of brain natriuretic peptide ($r = 0.37$), and 6-minute walk distance ($r = -0.28$). Over a median follow-up of 24 months, there were 34 combined cardiac events (30 hospitalizations for heart failure and 4 cardiac deaths). Patients with an ECV above the median were more likely to experience a cardiac event and ECV was independently associated with outcomes among imagine parameters in multivariate Cox-Regression analysis (HR, 1.01; CI, 1.01–1.20; $P = .049$). While ECV was markedly elevated in patients who had an event ($31.0\% \pm 4.6\%$ vs $28.5\% \pm 3.4\%$; $P > .01$), native T_1 -times did not differ ($P = .13$) in comparison with those in patients not reaching the combined endpoint. According to Kaplan-Meier analysis, the prognostic power of ECV seemed highest in the first 6 months of follow-up. Considering relevant clinical and hemodynamic parameters in a multivariate model, right ventricular end-diastolic volume ($P < .001$) and pulmonary vascular resistance ($P = .002$), but not ECV ($P = .978$) were found to be predictive of outcomes.

A link between hemodynamic alterations related to decreased LV compliance and diffuse myocardial fibrosis was established by Ellims et al.⁴⁵ They examined 20 cardiac transplant recipients referred for a clinically-indicated cardiac catheterization using invasive pressure volume loop measurement, CMR T₁ mapping with VAST sequences and echocardiography. Both postcontrast T₁ ($r = -0.71$; $P < .01$) time and ECV ($r = 0.58$; $P = .04$) significantly correlated with the load-independent myocardial stiffness constant (Beta). After correction for other parameters, the correlation of postcontrast T₁ time and Beta persisted on multivariate analysis. The implication of a causative link between the amount of fibrosis and stiffness is further strengthened by the biopsy-proven correlation of postcontrast T₁ times with actual fibrosis in cardiac transplant recipients.⁶⁴

Of note, no other clinical, hemodynamic, or echocardiographic parameter showed an association with pressure-volume loop-derived passive stiffness. Similarly, the time constant of isovolumic relaxation (Tau) showed no correlation with CMR measurements, or other parameters related to patient characteristics, hemodynamics, or imaging. Although the suggested concept of changes in cardiac structure causing functional alterations appears straightforward, its transferability to an HFpEF population seem at the least problematic, as predominantly relatively young, male cardiac transplant patients with hardly any HF symptoms or signs of diastolic dysfunction and only mildly elevated filling pressures were examined.

More recently, our group reported on the relationship between hemodynamics and CMR assessment in HFpEF patients, rigorously identified on the basis of the European consensus criteria.¹³ Twenty-four patients with HFpEF were compared with 12 control patients, who presented for evaluation of atypical chest pain, accompanied by a substantial cardiovascular risk profile, but without HF symptoms. Pressure-volume loops were acquired during baseline conditions, hand-grip exercise, and transient preload reduction by balloon occlusion of the inferior vena cava. In addition to load-independent myocardial diastolic stiffness and end-systolic elastance, measures of active relaxation (Tau), arterial elastance, and end-diastolic pressure volume relations (EDPVR) were derived at baseline and in response to handgrip exercise. T₁ mapping with ECV determination was performed using the MOLLI technique with assessment of native T₁ (precontrast) and postcontrast T₁ was acquired 15 minutes after gadolinium contrast administration, which allowed for the calculation of ECV.

Overall, ECV correlated highly with myocardial stiffness ($r = 0.75$; $P < .01$) and HFpEF patients showed elevated ECV ($33\% \pm 3\%$ vs $29\% \pm 3\%$; $P < .01$), whereas native T₁ ($P = .20$) and postcontrast T₁ times ($P = .08$) did not differ between groups. Adjusted for other imaging parameters (E/E' and LA volume), ECV remained the only independent predictor of beta in a multivariate model, suggesting a diagnostic value of ECV in HFpEF independent of echocardiographic assessment. Native T₁ times, but not ECV, correlated with Tau under exertion, indicating that

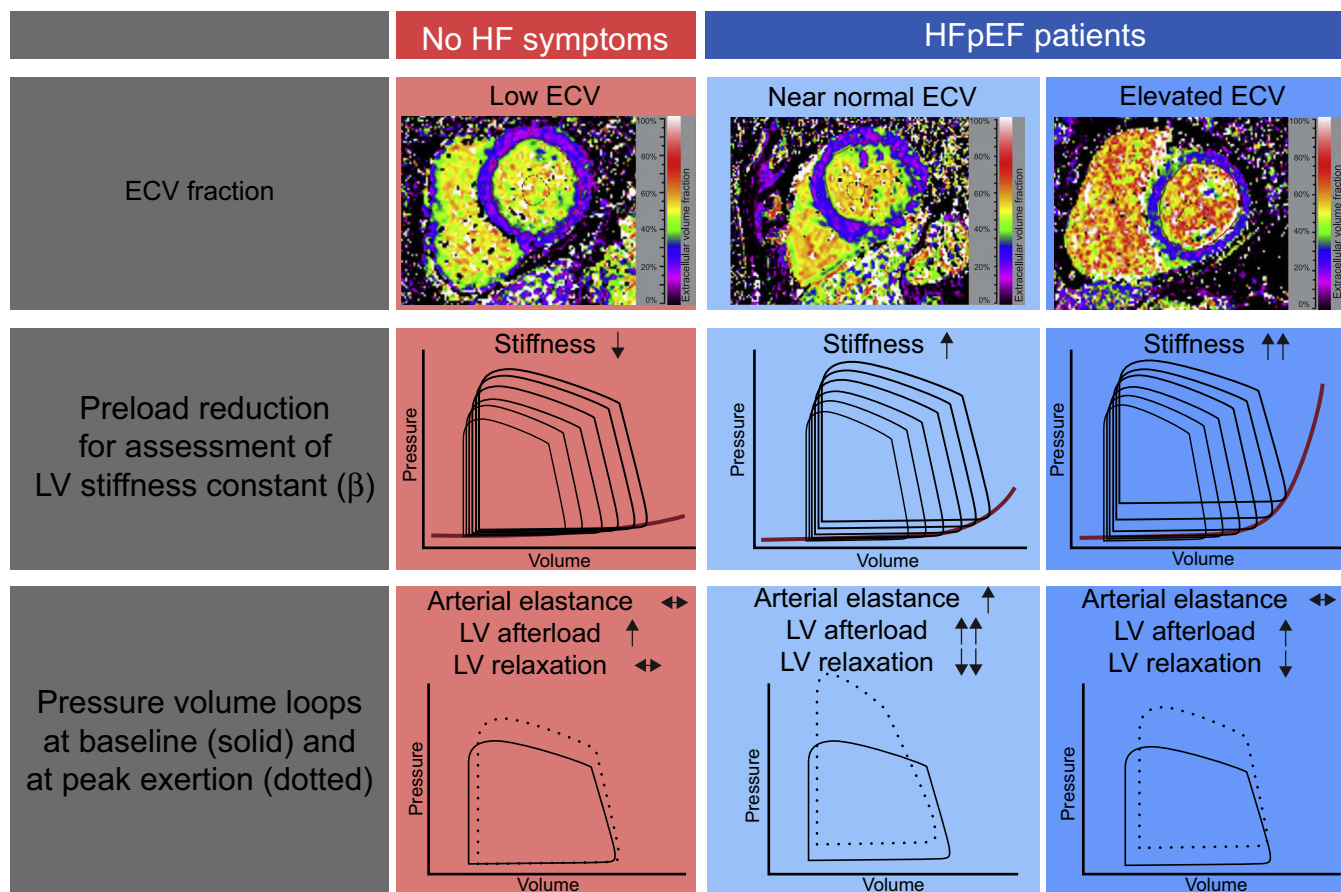


Figure 4. Overview of the results of the Left Ventricular Stiffness vs Fibrosis Quantification by T₁ mapping in Heart Failure With Preserved Ejection Fraction (STIFFMAP) trial.¹² While HFpEF patients demonstrated overall higher ECV, an elevated left ventricular stiffness constant, prolonged relaxation and a pathological rise of the end-diastolic pressure volume relations under exercise were found. After stratification according to the ECV median, in the HFpEF group with near normal ECV values, this was found to be caused predominantly by an elevated arterial stiffness, a marked hypertensive reaction to exercise and prolonged active relaxation. In the HFpEF group with the highest ECV, pronounced ventricular stiffening predominantly caused the pathological hemodynamic exercise response. ECV, extracellular volume; HF, heart failure; HFpEF, heart failure with preserved ejection fraction; LV, left ventricular.

fibrosis is likely more related to reduced myocardial compliance than to impaired myocardial relaxation.

Heart failure with preserved ejection fraction patients demonstrated more unfavorable hemodynamics with higher filling pressures, prolonged diastolic relaxation and a higher change of EDPVR from baseline to exercise. Additionally, ECV allowed for the identification of 2 patient groups, which demonstrated different underlying mechanisms for the development of diastolic dysfunction and exercise intolerance (Figure 4). Dividing the HFpEF cohort on the basis of median ECV, there were no differences in baseline characteristics, exercise testing, or echocardiographic measures of diastolic function between the groups. However, patients with ECV > median showed significantly higher myocardial stiffness values, whereas in patients with ECV < median, higher vascular load with impaired active relaxation were responsible for a similar unfavorable EDPVR change under exertion.

Thus, ECV was suggested not only to be predictive of increased myocardial stiffness, but also to allow the identification of patients who are more likely to have an alternative mechanism of diastolic dysfunction. In this particular setting, these patients showed elevated vascular load, most likely a result of arterial stiffening and late systolic reflection waves.⁶⁵

CONCLUSIONS

The emerging technique of CMR T₁ mapping has introduced the option to noninvasively characterize myocardial tissue to an extent that was previously only achievable with myocardial biopsies. Of special interest is the possibility to quantify myocardial extracellular changes. Increased diffuse myocardial fibrosis, usually undetectable with other imaging techniques, is a cornerstone of HFpEF pathophysiology and therefore patient characterization using T₁ mapping seems especially appealing in this patient group. Existing data support this notion as a relationship of measured T₁ times, and echocardiographically assessed diastolic function has been established in cardiovascular conditions known to be associated with myocardial fibrosis. In HFpEF especially, post-contrast measures, known to be more specific to the extracellular space, seem to be of greatest diagnostic value. Accordingly, HFpEF patients have been demonstrated to have higher ECVs than patients without HF, but lower ECVs than patients with HFrEF. Postcontrast T₁ times have also been suggested to be elevated in HFpEF and to be related to adverse pulmonary hemodynamic remodeling. Postcontrast T₁ times and ECV were found to be independently associated with clinical outcomes in this patient group. Hemodynamically, ECV has been shown to correlate with slower LV diastolic filling. Additionally, both ECV and postcontrast times correlate with myocardial stiffness, as assessed by pressure volume relations, providing complementary information to echocardiography. Finally, in 1 study, HFpEF patients could be stratified according to their ECV to noninvasively distinguish myocardial stiffness on the one hand and elevated arterial load with impaired active relaxation on the other hand as a leading determinant of their diastolic functional impairment.

Patient stratification according to their ECV might therefore be a suitable approach to partly unravel the heterogeneity of the HFpEF cohort, a notion that becomes even more attractive considering that viable treatment options for identified subgroups might readily be available (eg, antifibrotic neurohormal modulation with spironolactone or sacubitril).

To date, T₁ mapping data in HFpEF are still limited and existing trials share important limitations, such as small sample sizes, single center designs, and the lack of incorporating diastolic stress testing in most studies. Although a pathophysiologically plausible link exists between T₁ measures and interstitial fibrosis in HFpEF,

the role of myocardial factors confounding this relation needs to be further illuminated. Comparisons between studies are hampered by different protocols and imaging techniques. In conclusion, CMR T₁ has the potential to be an effective tool for patient characterization in large-scale epidemiological, diagnostic, and therapeutic HFpEF trials beyond traditional imaging parameters. Further efforts to standardize imaging techniques need to provide the basis for multicenter application.

CONFLICTS OF INTEREST

None declared.

REFERENCES

- Mozaffarian D, Benjamin EJ, Go AS, et al. Heart disease and stroke statistics—2015 update: A report from the American Heart Association. *Circulation*. 2015;131:e29–e322.
- Farmakis D, Parissis J, Lekakis J, Filippatos G. Acute Heart Failure: Epidemiology, Risk Factors, and Prevention. *Rev Esp Cardiol*. 2015;68:245–248.
- Owan TE, Hodge DO, Herges RM, Jacobsen SJ, Roger VL, Redfield MM. Trends in prevalence and outcome of heart failure with preserved ejection fraction. *N Engl J Med*. 2006;355:251–259.
- McMurray JJ, Packer M, Desai AS, et al. Angiotensin-neprilysin inhibition versus enalapril in heart failure. *N Engl J Med*. 2014;371:993–1004.
- Shah SJ, Kitzman DW, Borlaug BA, et al. Phenotype-specific treatment of heart failure with preserved ejection fraction: A multiorgan roadmap. *Circulation*. 2016;134:73–90.
- Paulus WJ, Tschope C, Sanderson JE, et al. How to diagnose diastolic heart failure: A consensus statement on the diagnosis of heart failure with normal left ventricular ejection fraction by the heart failure and echocardiography associations of the European Society of Cardiology. *Eur Heart J*. 2007;28:2539–2550.
- Zile MR, Gaasch WH, Anand IS, et al. Mode of death in patients with heart failure and a preserved ejection fraction: Results from the Irbesartan in Heart Failure With Preserved Ejection Fraction Study (I-Preserve) trial. *Circulation*. 2010;121:1393–1405.
- Persson H, Lonn E, Edner M, et al. Diastolic dysfunction in heart failure with preserved systolic function: Need for objective evidence: Results from the CHARM echocardiographic substudy-CHARMES. *J Am Coll Cardiol*. 2007;49:687–694.
- Kraigher-Krainer E, Shah AM, Gupta DK, et al. Impaired systolic function by strain imaging in heart failure with preserved ejection fraction. *J Am Coll Cardiol*. 2014;63:447–456.
- Borlaug BA, Paulus WJ. Heart failure with preserved ejection fraction: Pathophysiology, diagnosis, and treatment. *Eur Heart J*. 2011;32:670–679.
- Borlaug BA, Nishimura RA, Sorajja P, Lam CS, Redfield MM. Exercise hemodynamics enhance diagnosis of early heart failure with preserved ejection fraction. *Circ Heart Fail*. 2010;3:588–595.
- Kosmala W, Rojek A, Przewlocka-Kosmala M, Mysiak A, Karolko B, Marwick TH. Contributions of nondiastolic factors to exercise intolerance in heart failure with preserved ejection fraction. *J Am Coll Cardiol*. 2016;67:659–670.
- Rommel KP, von Roeder M, Latuscynski K, et al. Extracellular volume fraction for characterization of patients with heart failure and preserved ejection fraction. *J Am Coll Cardiol*. 2016;67:1815–1825.
- Shah SJ, Katz DH, Selvaraj S, et al. Phenomapping for novel classification of heart failure with preserved ejection fraction. *Circulation*. 2015;131:269–279.
- Lam CS, Roger VL, Rodeheffer RJ, Borlaug BA, Enders FT, Redfield MM. Pulmonary hypertension in heart failure with preserved ejection fraction: A community-based study. *J Am Coll Cardiol*. 2009;53:1119–1126.
- Melenovsky V, Hwang SJ, Lin G, Redfield MM, Borlaug BA. Right heart dysfunction in heart failure with preserved ejection fraction. *Eur Heart J*. 2014;35:3452–3462.
- Mohammed SF, Hussain I, AbouEzzeddine OF, et al. Right ventricular function in heart failure with preserved ejection fraction: A community-based study. *Circulation*. 2014;130:2310–2320.
- Senni M, Paulus WJ, Gavazzi A, et al. New strategies for heart failure with preserved ejection fraction: The importance of targeted therapies for heart failure phenotypes. *Eur Heart J*. 2014;35:2797–2815.
- Leong DP, De Pasquale CG, Selvanayagam JB. Heart failure with normal ejection fraction: The complementary roles of echocardiography and CMR imaging. *JACC Cardiovasc Imaging*. 2010;3:409–420.
- Flachskampf FA, Biering-Sorensen T, Solomon SD, Duvernoy O, Bjerner T, Smiseth OA. Cardiac imaging to evaluate left ventricular diastolic function. *JACC Cardiovasc Imaging*. 2015;8:1071–1093.
- Mewton N, Liu CY, Croisille P, Bluemke D, Lima JA. Assessment of myocardial fibrosis with cardiovascular magnetic resonance. *J Am Coll Cardiol*. 2011;57:891–903.
- Rommel KP, Badarni H, Desch S, et al. QRS complex distortion (Grade 3 ischaemia) as a predictor of myocardial damage assessed by cardiac magnetic resonance

- imaging and clinical prognosis in patients with ST-elevation myocardial infarction. *Eur Heart J Cardiovasc Imaging*. 2016;17:194–202.
23. Rommel KP, Baum A, Mende M, et al. Prognostic significance and relationship of worst lead residual ST segment elevation with myocardial damage assessed by cardiovascular MRI in myocardial infarction. *Heart*. 2014;100:1257–1263.
 24. Puntmann VO, Peker E, Chandrashekar Y, Nagel E. T1 mapping in characterizing myocardial disease: A comprehensive review. *Circ Res*. 2016;119:277–299.
 25. Sanz J, LaRocca G, Mirelis JG. Myocardial mapping with cardiac magnetic resonance: The diagnostic value of novel sequences. *Rev Esp Cardiol*. 2016;69:849–861.
 26. Paulus WJ, Tschope C. A novel paradigm for heart failure with preserved ejection fraction: Comorbidities drive myocardial dysfunction and remodeling through coronary microvascular endothelial inflammation. *J Am Coll Cardiol*. 2013;62:263–271.
 27. Zile MR, Baicu CF, Ikonomidis JS, et al. Myocardial stiffness in patients with heart failure and a preserved ejection fraction: Contributions of collagen and titin. *Circulation*. 2015;131:1247–1259.
 28. Zile MR, Baicu CF, Gaasch WH. Diastolic heart failure—abnormalities in active relaxation and passive stiffness of the left ventricle. *N Engl J Med*. 2004;350:1953–1959.
 29. Westermann D, Lindner D, Kasner M, et al. Cardiac inflammation contributes to changes in the extracellular matrix in patients with heart failure and normal ejection fraction. *Circ Heart Fail*. 2011;4:44–52.
 30. van Heerebeek L, Hamdani N, Handoko ML, et al. Diastolic stiffness of the failing diabetic heart: Importance of fibrosis, advanced glycation end products, and myocyte resting tension. *Circulation*. 2008;117:43–51.
 31. Kasner M, Westermann D, Lopez B, et al. Diastolic tissue Doppler indexes correlate with the degree of collagen expression and cross-linking in heart failure and normal ejection fraction. *J Am Coll Cardiol*. 2011;57:977–985.
 32. van Heerebeek L, Borbely A, Niessen HW, et al. Myocardial structure and function differ in systolic and diastolic heart failure. *Circulation*. 2006;113:1966–1973.
 33. Borbely A, Falcao-Pires I, van Heerebeek L, et al. Hypophosphorylation of the stiff n2b titin isoform raises cardiomyocyte resting tension in failing human myocardium. *Circ Res*. 2009;104:780–786.
 34. Mohammed SF, Hussain S, Mirzoyev SA, Edwards WD, Maleszewski JJ, Redfield MM. Coronary microvascular rarefaction and myocardial fibrosis in heart failure with preserved ejection fraction. *Circulation*. 2015;131:550–559.
 35. Tschope C, Paulus WJ. Is echocardiographic evaluation of diastolic function useful in determining clinical care? Doppler echocardiography yields dubious estimates of left ventricular diastolic pressures. *Circulation*. 2009;120:810–820.
 36. Westermann D, Kasner M, Steendijk P, et al. Role of left ventricular stiffness in heart failure with normal ejection fraction. *Circulation*. 2008;117:2051–2060.
 37. Kass DA, Bronzwaer JG, Paulus WJ. What mechanisms underlie diastolic dysfunction in heart failure? *Circ Res*. 2004;94:1533–1542.
 38. Taylor AJ, Salerno M, Dharmakumar R, Jerosch-Herold M. T1 mapping: Basic techniques and clinical applications. *JACC Cardiovasc Imaging*. 2016;9:67–81.
 39. Ugander M, Oki AJ, Hsu LY, et al. Extracellular volume imaging by magnetic resonance imaging provides insights into overt and sub-clinical myocardial pathology. *Eur Heart J*. 2012;33:1268–1278.
 40. Broberg CS, Chugh SS, Conklin C, Sahn DJ, Jerosch-Herold M. Quantification of diffuse myocardial fibrosis and its association with myocardial dysfunction in congenital heart disease. *Circ Cardiovasc Imaging*. 2010;3:727–734.
 41. Messroghli DR, Radjenovic A, Kozerke S, Higgins DM, Sivanathan MU, Ridgway JP. Modified look-locker inversion recovery (MOLLI) for high-resolution T1 mapping of the heart. *Magn Reson Med*. 2004;52:141–146.
 42. Piechnik SK, Ferreira VM, Dall'Armellina E, et al. Shortened Modified Look-Locker Inversion recovery (shMOLLI) for clinical myocardial T1-mapping at 1.5 and 3 T within a 9 heartbeat breathhold. *J Cardiovasc Magn Reson*. 2010;12:69.
 43. Chow K, Flewitt JA, Green JD, Pagano JJ, Friedrich MG, Thompson RB. Saturation recovery single-shot acquisition (SASHA) for myocardial T(1) mapping. *Magn Reson Med*. 2014;71:2082–2095.
 44. Roujol S, Weingartner S, Foppa M, et al. Accuracy, precision, and reproducibility of four T1 mapping sequences: A head-to-head comparison of MOLLI, shMOLLI, SASHA, and sapphire. *Radiology*. 2014;272:683–689.
 45. Ellims AH, Shaw JA, Stub D, et al. Diffuse myocardial fibrosis evaluated by post-contrast T1 mapping correlates with left ventricular stiffness. *J Am Coll Cardiol*. 2014;63:1112–1118.
 46. Mascherbauer J, Marzluft BA, Tufaro C, et al. Cardiac magnetic resonance post-contrast T1 time is associated with outcome in patients with heart failure and preserved ejection fraction. *Circ Cardiovasc Imaging*. 2013;6:1056–1065.
 47. Shi X, Kim SE, Jeong EK. Single-shot T1 mapping using simultaneous acquisitions of spin- and stimulated-echo-planar imaging (2D ss-SESTEPI). *Magn Reson Med*. 2010;64:734–742.
 48. Warntjes MJ, Kihlberg J, Engvall J. Rapid T1 quantification based on 3D phase sensitive inversion recovery. *BMC Med Imaging*. 2010;10:19.
 49. Kellman P, Hansen MS. T1-mapping in the heart: Accuracy and precision. *J Cardiovasc Magn Reson*. 2014;16:2.
 50. Lurz P, Luecke C, Eitel I, et al. Comprehensive Cardiac Magnetic Resonance Imaging in Patients With Suspected Myocarditis: The MyoRacer-Trial. *J Am Coll Cardiol*. 2016;67:1800–1811.
 51. Lurz P, Lang D, Luecke C, et al. Cardiac magnetic resonance derived extracellular volume fraction estimates myocardial fibrosis in patients with cardiomyopathy without inflammation but not in presence of significant inflammation [Abstract]. *Eur J Heart Fail*. 2016;18 Suppl 1:153.
 52. Wong TC, Piehler K, Meier CG, et al. Association between extracellular matrix expansion quantified by cardiovascular magnetic resonance and short-term mortality. *Circulation*. 2012;126:1206–1216.
 53. Banyersad SM, Fontana M, Maestrini V, et al. T1 mapping and survival in systemic light-chain amyloidosis. *Eur Heart J*. 2015;36:244–251.
 54. Schelbert EB, Piehler KM, Zareba KM, et al. Myocardial fibrosis quantified by extracellular volume is associated with subsequent hospitalization for heart failure, death, or both across the spectrum of ejection fraction and heart failure stage. *J Am Heart Assoc*. 2015;4:e002613.
 55. Puntmann VO, Carr-White G, Jabbour A, et al. T1-mapping and outcome in nonischemic cardiomyopathy: All-cause mortality and heart failure. *JACC Cardiovasc Imaging*. 2016;9:40–50.
 56. Kammerlander AA, Marzluft BA, Zotter-Tufaro C, et al. T1 mapping by CMR imaging: From histological validation to clinical implication. *JACC Cardiovasc Imaging*. 2016;9:14–23.
 57. Moon JC, Messroghli DR, Kellman P, et al. Myocardial T1 mapping and extracellular volume quantification: A Society for Cardiovascular Magnetic Resonance (SCMR) and CMR Working Group of the European Society of Cardiology consensus statement. *J Cardiovasc Magn Reson*. 2013;15:92.
 58. Captur G, Gatehouse P, Keenan KE, et al. A medical device-grade T1 and ECV phantom for global T1 mapping quality assurance—the T1 mapping and ECV standardization in cardiovascular magnetic resonance (T1MES) program. *J Cardiovasc Magn Reson*. 2016;18:58.
 59. Ellims AH, Iles LM, Ling LH, Hare JL, Kaye DM, Taylor AJ. Diffuse myocardial fibrosis in hypertrophic cardiomyopathy can be identified by cardiovascular magnetic resonance, and is associated with left ventricular diastolic dysfunction. *J Cardiovasc Magn Reson*. 2012;14:76.
 60. Karamitsos TD, Piechnik SK, Banyersad SM, et al. Noncontrast T1 mapping for the diagnosis of cardiac amyloidosis. *JACC Cardiovasc Imaging*. 2013;6:488–497.
 61. Jellis C, Wright J, Kennedy D, et al. Association of imaging markers of myocardial fibrosis with metabolic and functional disturbances in early diabetic cardiomyopathy. *Circ Cardiovasc Imaging*. 2011;4:693–702.
 62. Su MY, Lin LY, Tseng YH, et al. CMR-verified diffuse myocardial fibrosis is associated with diastolic dysfunction in HFPeF. *JACC Cardiovasc Imaging*. 2014;7:991–997.
 63. Duca F, Kammerlander AA, Zotter-Tufaro C, et al. Interstitial Fibrosis, Functional Status, and Outcomes in Heart Failure With Preserved Ejection Fraction Insights From a Prospective Cardiac Magnetic Resonance Imaging Study. *Circ Cardiovasc Imaging*. 2016;9:e005277.
 64. Iles L, Pfluger H, Phrommintikul A, et al. Evaluation of diffuse myocardial fibrosis in heart failure with cardiac magnetic resonance contrast-enhanced T1 mapping. *J Am Coll Cardiol*. 2008;52:1574–1580.
 65. Leite-Moreira AF, Correia-Pinto J. Load as an acute determinant of end-diastolic pressure-volume relation. *Am J Physiol Heart Circ Physiol*. 2001;280:H51–H59.